

# GFD 2017 Lecture 8: Testing the Ocean Trigger Hypothesis for Greenland's Recent Glacier Retreat

Fiamma Straneo; notes by Eric Hester and Jessica Kenigson

June 28, 2017

## 1 Testing the Ocean Trigger Hypothesis for Greenland's Glaciers

### 1.1 Establishing rates of mass loss in Greenland

The change in mass  $M$  of an ice sheet with respect to time is given by

$$\frac{dM}{dt} = SMB - D \quad (1)$$

where  $SMB$  represents the surface mass balance and  $D$  represents the rate of ice discharge. Here  $SMB$  is the difference between the rate of accumulation due to precipitation and the rate of ablation due to surface melt and sublimation, while  $D$  represents the rate of loss due to glacial calving and melting at the ice margins by the ocean. In order to accurately monitor and predict the ice sheet mass balance in a changing climate, it is necessary to isolate  $SMB$  and  $D$ . In Antarctica, mass loss occurs primarily through  $D$  (as ambient temperatures are too low to permit significant mass loss from surface melting); in Greenland this is not the case.

Since 2002, GRACE satellite observations of Greenland mass balance changes through gravimetry have provided data on an ice-sheet-wide scale. Figure 1 shows the cumulative mass change of the ice sheet since 2002 as resolved by GRACE. The declining mass is superimposed upon a significant seasonal cycle of  $SMB$ .

Prior to GRACE, ice mass changes were necessarily interpolated from scattered in situ observations. Greenland  $SMB$  has been relatively adequately monitored since  $\sim 1980$ . In order to obtain estimates for earlier periods, Greenland Ice Sheet  $SMB$  is reconstructed from (typically) atmospheric and snow-pack models. The Regional Atmospheric Climate Model (RACMO) simulates the spatial distribution of climatological  $SMB$  from 1958 – 2007 [3]. Spatially,  $SMB$  is  $\mathcal{O}(1000 \text{ kg m}^{-2} \text{ yr}^{-1})$  along the coast of southeast Greenland due to significant orographic precipitation. Over much of northern Greenland,  $SMB$  is  $\mathcal{O}(100 \text{ kg m}^{-2} \text{ yr}^{-1})$  due to the relatively low precipitation rates in the interior (and by relatively cold temperatures at high latitudes). Over the coastal margin of southwest Greenland,  $SMB$  can reach  $\mathcal{O}(-1000 \text{ kg m}^{-2} \text{ yr}^{-1})$ , which is attributable to significant surface melting.



Figure 1: Monthly change in mass of Greenland from April 2002 – April 2016 (cumulative). Figure reproduced from <https://www.climate.gov/news-features/featured-images/greenland-ice-mass-loss-continued-2016>.

Measurements of  $D$  for a particular glacier are made via remote sensing of the ice velocity across a transect (fluxgate) as near as possible to the grounding line, and  $D$  is approximated by

$$D = VhH \quad (2)$$

where  $V$  is the velocity perpendicular to the transect,  $h$  is the width of the fluxgate, and  $H$  is the depth of the glacier [5, 2]. Typically,  $D$  is assumed to be seasonally invariant (due both to a paucity of observations and, when observations have been available, a lack of evidence of a clear seasonal dependence). In one study,  $D$  was calculated at 178 outlet glaciers [2];  $V$  was estimated (where possible) by repeat imaging from the Landsat 7 Enhanced Thematic Mapper Plus and the Advanced Spaceborne Thermal and Reflectance Radiometer (ASTER). In addition,  $H$  was obtained from digital elevation models (DEMs) by differencing the bed elevation from the surface elevation (where possible; bed elevation data was not available in the cross-flow direction at all glaciers).

Historical reconstructions of the total mass balance ( $TMB$ , defined as  $SMB - D$ ) require estimates of  $D$ , which are often based upon correlations between  $SMB$  and  $D$  over periods in which both quantities have been observed. Figure 2 shows a reconstruction of the Greenland Ice Sheet  $SMB$ ,  $D$ , and  $TMB$  from 1900 – 2010 [6]. The historical reconstruction is based upon differences between the maximum extent of the ice sheet during the Little Ice Age (as inferred from trimlines and moraines) and aerial photogrammetry from 1978-1987, which allows the change in elevation around the entire perimeter of the ice sheet to be calculated. This is then interpolated to the interior.  $SMB$  modeling is used to resolve the mass balance

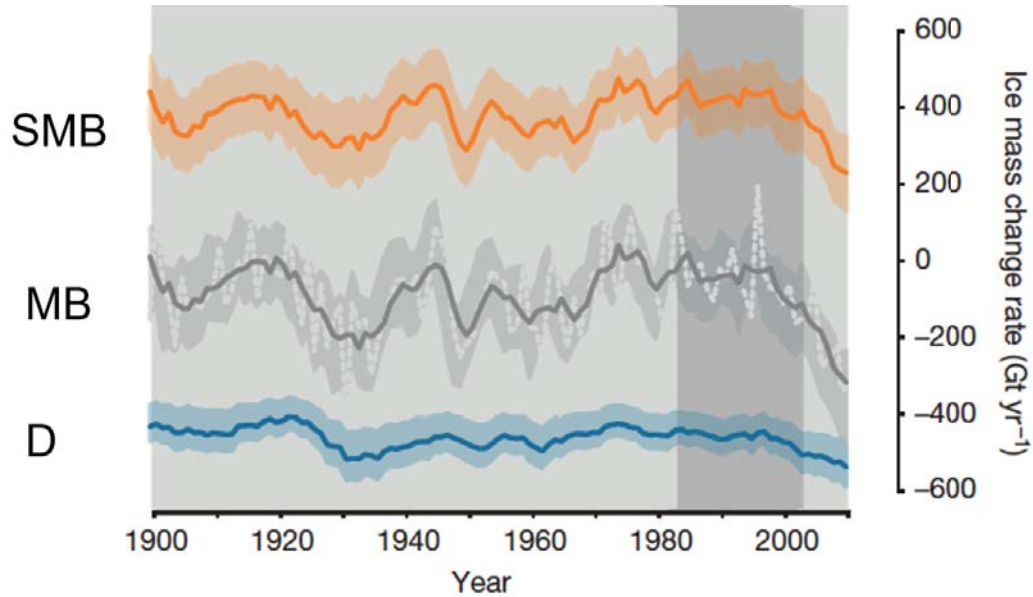


Figure 2: Five-year mean of  $SMB$  (orange line), modeled ice discharge (blue line), and 5-year mean of total mass balance (gray) with  $1\sigma$  uncertainty range (shading). Figure subsetted from [6].

into components arising from  $SMB$  and  $D$  (see their “Methods” section). Mass loss is seen to significantly accelerate around  $\sim 1990$ , with mass balance deficits increasing at a rate not seen since perhaps  $\sim 1920$ – $1930$ . What might account for the accelerated mass loss since  $\sim 1990$ ?

## 1.2 Ocean trigger hypothesis

Changes in both  $SMB$  and  $D$  contribute in approximately equal part to the mass loss from the Greenland Ice Sheet since  $\sim 1990$ . Moreover, an accelerated retreat of large outlet glaciers beginning around  $\sim 2000$  (primarily around the western and southern coast of Greenland) has been documented.

Two major types of glaciers exist along the margins of Greenland: “floating ice tongue” glaciers and tidewater glaciers. Tidewater glaciers are characterized by a relatively shear vertical face and primarily lose mass through glacial calving, while floating ice tongue glaciers are characterized by a long, thin, floating ice protrusion into the ocean from the grounding line and primarily lose mass through melting. Many of Greenland’s large tidewater glaciers (including, for example, Jacobskavn Isbrae, Helheim, and Zachariae Isstrom) had floating ice tongues in the recent past.

The ocean trigger hypothesis [13] suggests that the glacier retreat beginning around  $\sim 2000$  (Figure 3) and contributing to the relative increase of  $D$  (as in [6]) was initiated by oceanic drivers. The intrusion of anomalously warm ocean water onto the shelf causes submarine melting of the floating ice tongue, triggering rapid thinning and ungrounding, which reduces buttressing and causes acceleration and calving. For instance, Jacobshavn Isbrae transitioned from a regime of slow ice accumulation to rapid thinning beginning around

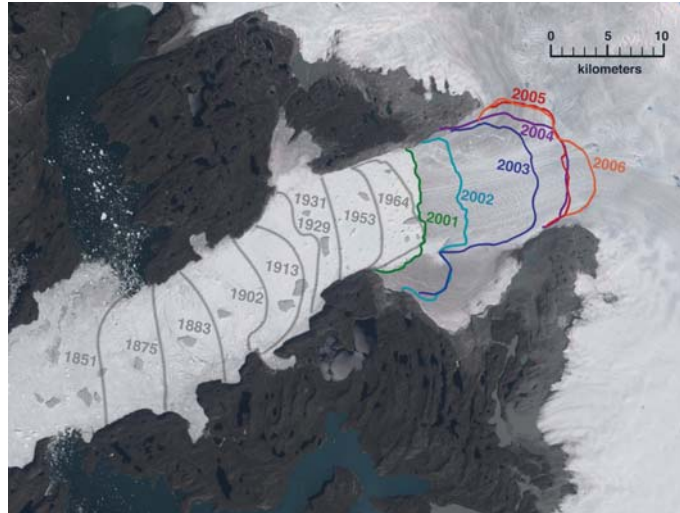


Figure 3: Shift in the calving front at Jacobshavn Isbrae from 1851-2006. Figure reproduced from <https://svs.gsfc.nasa.gov/3395>.

1997, and this was accompanied by an approximate doubling of velocity [4]. The accelerated mass loss is thought to be associated with warm oceanic inflow from the Irminger Sea. This is in contrast to the hypothesis that atmospheric warming causes enhanced surface melt and bed lubrication, leading to accelerated sliding. Hydrographic data in and around Greenland's fjords is difficult to obtain, particularly at depth. However, this warming signal beginning around 1997 (at depths of 150-600 m) was captured by trawl fishery measurements made from 1991 – 2006.

The ocean trigger hypothesis is supported by several independent lines of evidence. Indeed, ocean currents which bifurcate from the North Atlantic Current transport warm equatorial waters close to the southern coastal shelf of Greenland (Figure 5 shows a schematic diagram), suggesting that it is plausible for outlet glaciers to respond sensitively to changes in ocean temperature. However, few direct measurements of ocean temperature at depth along the shelf are available over the period of interest, requiring the use of sparse direct measurements, proxy data, and models. For instance, a numerical ice-flow model with a dynamic calving front has been used to study the reponse of Helheim glacier to various front-stress perturbations, changes in basal lubrication, and changes in the ablation rate [8]. Experiments with front-stress perturbations (which could occur due to rapid thinning of the floating ice tongue) best captured the observed rate of retreat and lend credence to the ocean trigger hypothesis.

Furthermore, paleoceanographic reconstructions fail to refute the ocean trigger hypothesis. For example, at Disko Bugt (West Greenland), a 100-year long (1910 – 2007) record of ocean temperature at approximately 300 m depth was reconstructed based upon the relative presence of warm and cold water taxa of benthic foraminifera in a series of sediment cores [7]. Indeed, the accelerated retreat of Jacobshavn Isbrae beginning after 1998 coincided with a period of ocean warming locally (and local ocean temperatures were related to the Atlantic Multidecadal Oscillation).

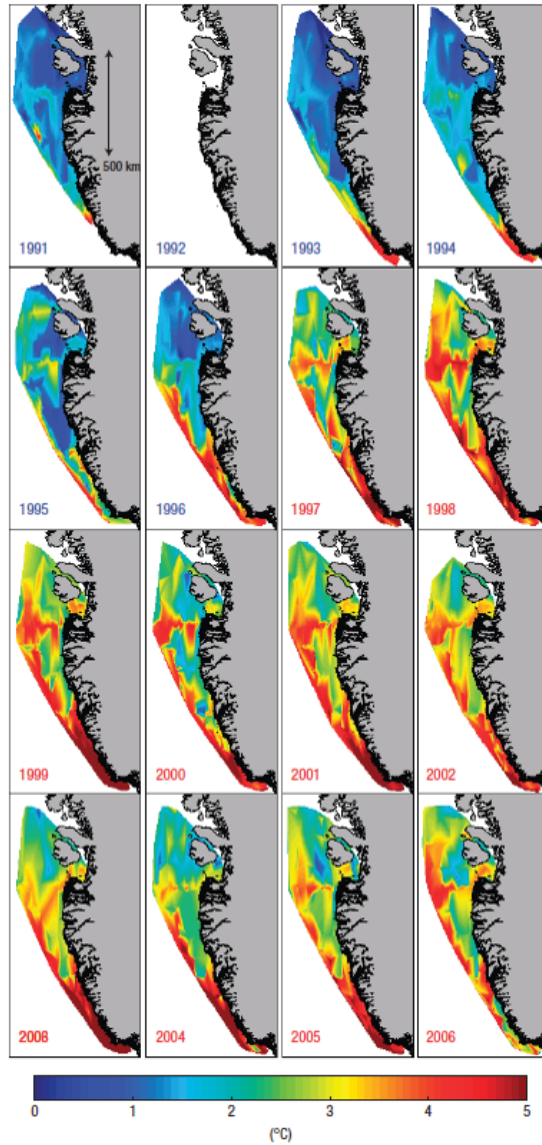


Figure 4: Depth-averaged temperature as obtained from trawl fisheries for 1991-2006 (150-600 m average). Note the increase in temperature near Jacobshavn Isbrae in 1997. Figure reproduced from [4].

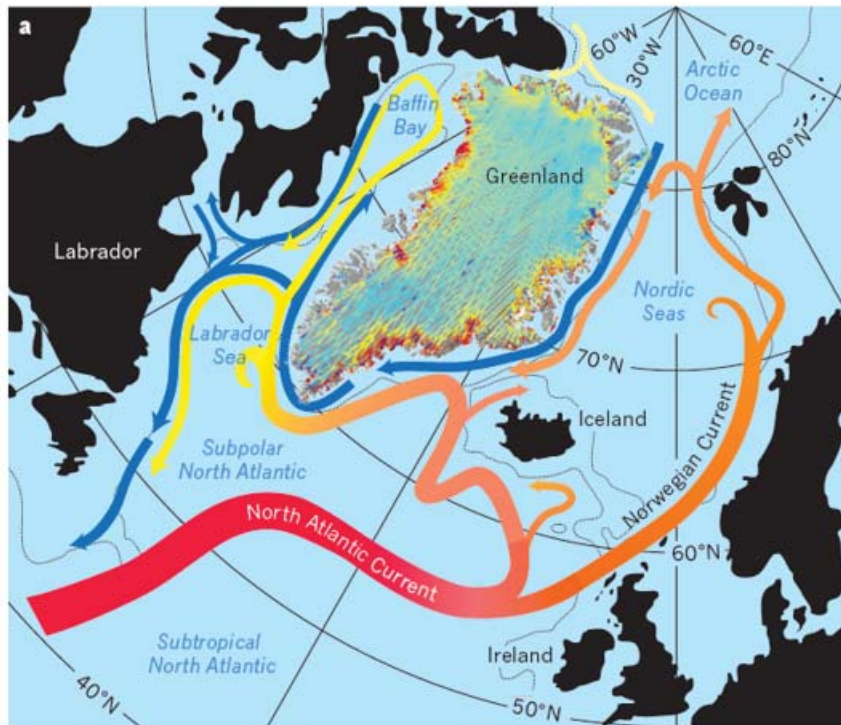


Figure 5: Schematic diagram of the ocean circulation around Greenland. Note the proximity of the warm Irminger Current (warm northward-flowing current branching from the North Atlantic Current to the west) to the coastal shelf of Greenland. Figure adapted from [13].

Calving rates may be reconstructed using the observation that icebergs are “dirty.” Specifically, Ice-Rafted Debris (IRD) deposited in Semilik Fjord near the Helheim Glacier terminus has been used as a proxy for glacial calving [1]. Based upon measurements from sediment cores, a record of the calving rate has been reconstructed from 1890 to near present. In particular, the sand fraction is used to represent the IRD since sand grains are likely to have been transported by icebergs rather than advected by meltwater plumes due to their large size (which causes them to rain out of suspension). The authors note that the accelerated calving event of the early 2000s (as well as a period during the early ~1930s – 1940s) was associated with warm phases of the Atlantic Multidecadal Oscillation (indicating that inflowing Atlantic waters were relatively warm) and with relatively low export of cold Arctic water. This supports the hypothesis that enhanced submarine melt at Helheim was triggered by contact with anomalously warm ocean water.

Indeed, the influx of cold Arctic water through the Fram Strait to the coastal margins of Greenland (as indicated by the Storis index, related to the latitude of the sea ice extent along the coast of southwest Greenland) versus the influx of relatively warm water from the south via the North Atlantic Current/Irminger Current (as given by a temperature transect south of Iceland) likely influences the calving rate [1]. For this reason, a “Shelf Index” is constructed as the sum of these indices, and the Shelf Index is seen to correlate with the calving rate on interannual and longer timescales ( $r = 0.41$  for 3-year mean, which is statistically significant at the 95% level). Correlations between the (negative) Storis index and Atlantic water temperatures as measured along the transect are nearly as strong, yet correlations with atmospheric variables such as the wintertime North Atlantic Oscillation index are also significant ( $r = -0.45$ ).

Thus, we see that there are multiple independent lines of evidence to support the Ocean Trigger hypothesis.

## 2 Ice-ocean Interactions in Greenland Glaciers

The evolution of Greenland glaciers depends on a range of complex phenomena, associated with changes in atmospheric and oceanic conditions on multiple spatial and temporal scales.

This lecture will outline the current understanding of the effect of oceanic forcing on Greenland glaciers, and the techniques used to establish these facts.

### 2.1 Greenland glaciers: tidewater vs tongues

There are two types of outlet glaciers in Greenland, characterised by their structure beyond their grounding line (the furthest point at which they are in contact with the sea bed).

The first and most common, tidewater glaciers, do not extend far beyond their grounding line, and display vigorous calving (iceberg production) at their edge. The other type, floating tongue glaciers, instead extend tens of kilometres beyond their grounding line. Further, floating ice tongues typically balance the incoming ice flux by melt, and do not strongly calve. Floating tongue glaciers are able to balance the incoming ice flux by melt as they have a much larger area in contact with the fjord waters.

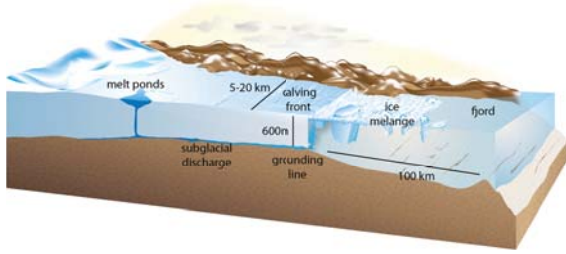


Figure 6: Schematic of typical Greenland tidewater glacier. Figure adapted from [14].

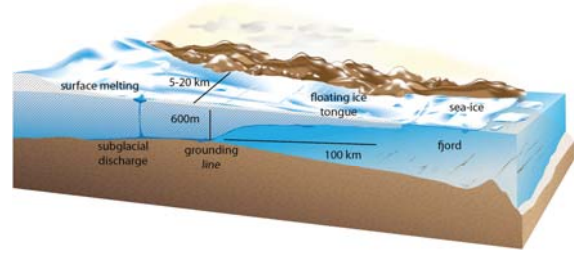


Figure 7: Floating tongue glaciers extend far beyond the grounding line. Figure adapted from [14].

## 2.2 Ocean water in fjords

The waters surrounding East Greenland are divided between two dominant water types - the warmer Atlantic water (AW) supplied by the North Atlantic current, and cooler polar water (PW) from the pole (Figure 8). The location of these waters, and in particular their interaction with glaciers when *within* the fjord, is believed to control glacial melting.

Straneo et. al. [12] performed ship and mooring based measurements of oceanographic data in Sermilik Fjord during 2008. They found the bottom of the fjord (beyond 200-300 m) was filled with warmer Atlantic water, while cooler polar water resided in the higher layers. These two modes were supplemented by a third water mass of glacial meltwater during the summer.

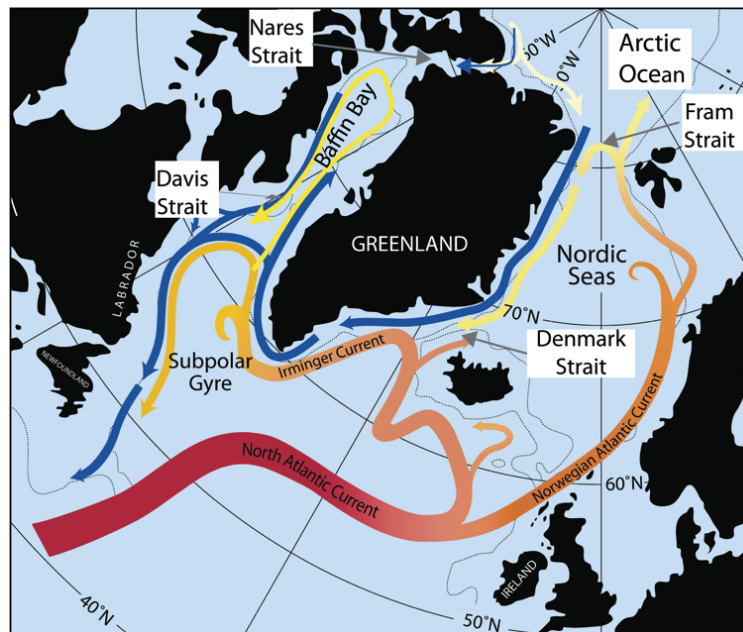


Figure 8: Schematic of ocean currents around Greenland. Figure from [10].

Importantly, they found that these waters were continuously replenished [12]. There are several mechanisms that contribute to this replacement, but one main driver of fjord/shelf

exchange is variations in the pycnocline on the shelf near the mouth of the fjord.

Figure 9 illustrates this mechanism with the example of Ekman transport by along coast winds. These winds (into the page) force transport of the surface layer toward the right (into the fjord), depressing the shelf pycnocline. The fjord waters then equilibrate to this new stratification by inflow of the top polar water, and outflow of the bottom Atlantic water. When the forcing ceases, the fjord waters will then relax to the original equilibrium, thereby replenishing the waters.

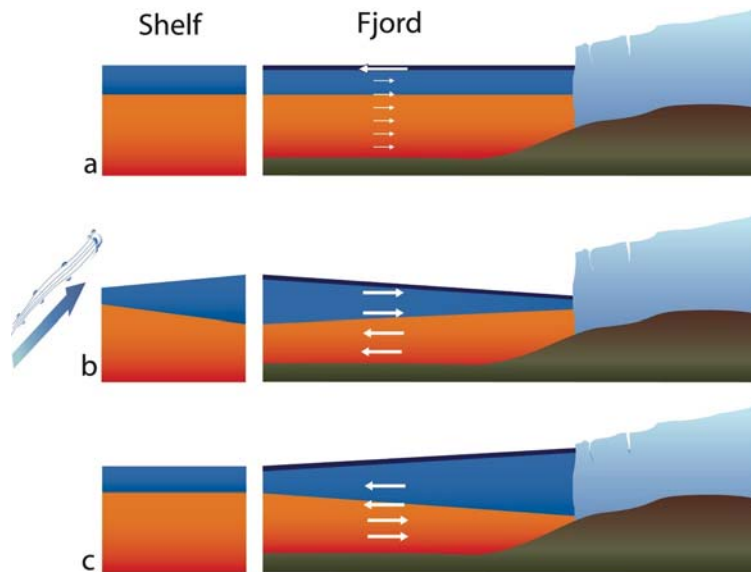


Figure 9: Wind driven forcing of shelf waters will adjust the shelf pycnocline, to which the fjord waters equilibrate. When the forcing ceases, the fjord waters readjust to the previous equilibrium (c). Figure adapted from [12] (Supplementary Information).

The presence of high sills in fjords may be able to block this transfer however [9, 16], mitigating the influence of the warmer Atlantic water.

### 2.3 Glacial melt from temperature-salinity diagrams

The distribution of fjord water characteristics is highly revealing when plotted on a (potential) Temperature ( $\theta$ ) - Salinity ( $S$ ) diagram. This is because when salt water melts ice, the properties of the water-ice mixture will evolve along a straight line in  $\theta - S$  space - as explained in Adrian Jenkins' first lecture. Water measurements close to the line imply the melting of glacial ice; divergence implies some other process is occurring (such as mixing with glacial runoff).

Straneo and others [11, 15] found that measurements around Greenland glaciers were consistent with melting of glaciers by Atlantic Water. The red curves in Figure 10 show  $\theta - S$  measurements of water near the fjord mouth, while the blue curves are near the glacier. The winter measurements (on the right), show that water near the glacier lies closer to the melting line of Atlantic water, implying that the water is melting the glacier.

The summer measurements tell a different story however. Now, the near-glacier water diverges from the melting line of the Atlantic water, instead being much fresher than expected. This is due to discharge, including at depth, of surface melt driven by a warm atmosphere above the ice.

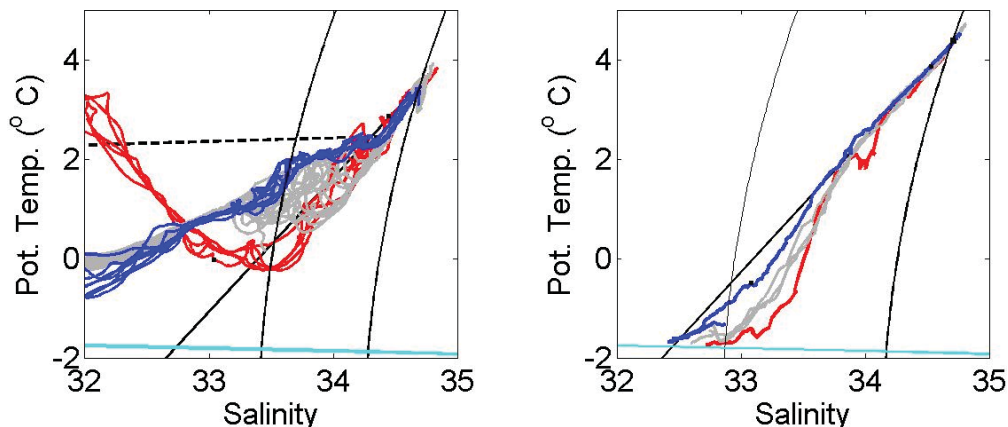


Figure 10:  $\theta - S$  measurements near Helheim glacier in summer (left) and winter (right). The red curves are of waters near the mouth of the fjord, and the blue readings are as close as possible to the glacier edge. The influence of the glacier is seen through the differences between the red and blue curves. The solid black line shows the melting line of Atlantic water, while the dashed line shows the line for mixing with glacial runoff. The curved lines are isopycnals, the cyan line shows the freezing temperature at zero pressure for varying salinities. Figure adapted from [11].

## 2.4 Lagrangian ice flux divergence measurements

The melting of ice tongues can be inferred by measuring the divergence of the ice flow. Assuming a vertically uniform velocity  $\mathbf{u} = (u, v)$  and density  $\rho_i$ , the melt rate  $\dot{a}$  of a floating ice tongue can be inferred from the conservation law for ice thickness  $h$ :

$$\frac{\partial h}{\partial t} + \nabla \cdot (h\mathbf{u}) = \frac{\partial h}{\partial t} + \mathbf{u} \cdot \nabla h + h\nabla \cdot \mathbf{u} = \dot{a}. \quad (3)$$

This Eulerian framework suffers from a key drawback however; for sparse sampling times, the calculation of time derivatives will be affected by *aliasing* – If the sampling time is too sparse and a second peak is in the same location as a past peak, then there is no way to infer a change in thickness of the ice.

A more effective approach is to switch to a Lagrangian framework, in which we track the time derivative of the ice thickness *following the ice*,  $Dh/Dt = \partial h/\partial t + \mathbf{u} \cdot \nabla h$ . By tracking the ice, we are able to minimize aliasing. This gives our conservation law as

$$\frac{Dh}{Dt} + h\nabla \cdot \mathbf{u} = \dot{a}. \quad (4)$$

Figure 10:  $\theta - S$  measurements near Helheim glacier in summer (left) and winter (right). The red curves are of waters near the mouth of the fjord, and the blue readings are as close as possible to the glacier edge. The influence of the glacier is seen through the differences between the red and blue curves. The solid black line shows the melting line of Atlantic water, while the dashed line shows the line for mixing with glacial runoff. The curved lines are isopycnals, the cyan line shows the freezing temperature at zero pressure for varying salinities. Figure adapted from [11].

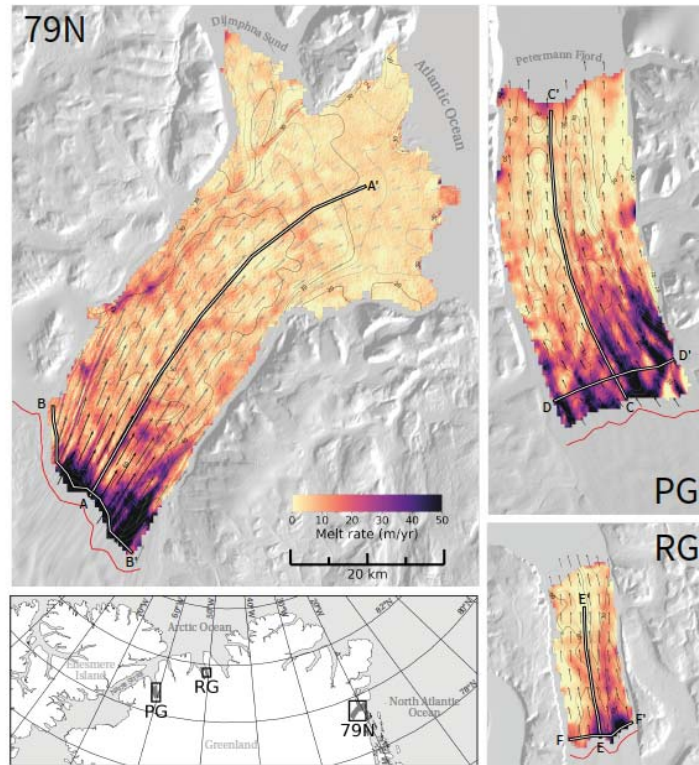


Figure 11: Greenland glacier melt rates determined using Lagrangian ice flux divergence measurements. Figure from [17].

The first step in estimating these quantities is to measure the surface elevation of the ice tongue using Digital Elevation Maps at multiple times.

The thickness of the ice tongue can be measured given knowledge of the tidal data, and assuming hydrostatic balance of the ice. The hydrostatic approximation becomes invalid within several kilometres of the grounding line, preventing the use of this technique in these areas.

By cross correlating successive elevation maps, the velocity of the ice  $\mathbf{u}$  can be inferred, and the elevation (thus thickness) change  $Dh/Dt$  can be measured. From these measurements, the total melt rate of the ice tongue can then be inferred. The submarine melting can finally be isolated by subtracting the surface melt using a model of atmospheric melting. Putting all this together, the subglacial melt of glaciers can be calculated, as seen in Figure 11 for three Greenland glaciers [17].

## References

- [1] C. S. ANDRESEN, F. STRANEO, M. H. RIBERGAARD, A. A. BJØRK, T. J. ANDERSEN, A. KUIJPERS, N. NØRGAARD-PEDERSEN, K. H. KJÆR, F. SCHJØTH,

- K. WECKSTRÖM, ET AL., *Rapid response of Helheim Glacier in Greenland to climate variability over the past century*, *Nature Geoscience*, 5 (2012), pp. 37–41.
- [2] E. M. ENDERLIN, I. M. HOWAT, S. JEONG, M.-J. NOH, J. H. ANGELEN, AND M. R. BROEKE, *An improved mass budget for the Greenland ice sheet*, *Geophysical Research Letters*, 41 (2014), pp. 866–872.
- [3] J. ETTEMA, M. R. VAN DEN BROEKE, E. VAN MEIJGAARD, W. J. VAN DE BERG, J. L. BAMBER, J. E. BOX, AND R. C. BALES, *Higher surface mass balance of the Greenland ice sheet revealed by high-resolution climate modeling*, *Geophysical Research Letters*, 36 (2009).
- [4] D. M. HOLLAND, R. H. THOMAS, B. DE YOUNG, M. H. RIBERGAARD, AND B. LYBERTH, *Acceleration of Jakobshavn Isbrae triggered by warm subsurface ocean waters*, *Nature geoscience*, 1 (2008), pp. 659–664.
- [5] I. M. HOWAT, I. JOUGHIN, AND T. A. SCAMBOS, *Rapid changes in ice discharge from Greenland outlet glaciers*, *Science*, 315 (2007), pp. 1559–1561.
- [6] K. K. KJELDSSEN, N. J. KORSGAARD, A. A. BJØRK, S. A. KHAN, S. FUNDER, N. K. LARSEN, J. L. BAMBER, W. COLGAN, M. VAN DEN BROEKE, M.-L. SIGGAARD-ANDERSEN, ET AL., *Spatial and temporal distribution of mass loss from the Greenland Ice Sheet since AD 1900*, *Nature*, 528 (2015), pp. 396–400.
- [7] J. LLOYD, M. MOROS, K. PERNER, R. J. TELFORD, A. KUIJPERS, E. JANSEN, AND D. MCCARTHY, *A 100 yr record of ocean temperature control on the stability of Jakobshavn Isbrae, West Greenland*, *Geology*, 39 (2011), pp. 867–870.
- [8] F. M. NICK, A. VIELI, I. M. HOWAT, AND I. JOUGHIN, *Large-scale changes in Greenland outlet glacier dynamics triggered at the terminus*, *Nature Geoscience*, 2 (2009), pp. 110–114.
- [9] F. SCHJOTH, C. S. ANDRESEN, F. STRANEO, T. MURRAY, K. SCHARRER, AND A. KORABLEV, *Campaign to map the bathymetry of a major Greenland fjord*, *Eos, Transactions American Geophysical Union*, 93 (2012), pp. 141–142.
- [10] F. STRANEO AND C. CENEDESE, *The dynamics of Greenland’s glacial fjords and their role in climate*, *Annual Review of Marine Science*, 7 (2015), pp. 89–112. PMID: 25149564.
- [11] F. STRANEO, R. G. CURRY, D. A. SUTHERLAND, G. S. HAMILTON, C. CENEDESE, K. VAGE, AND L. A. STEARNS, *Impact of fjord dynamics and glacial runoff on the circulation near Helheim Glacier*, *Nature Geosci*, 4 (2011), pp. 322–327.
- [12] F. STRANEO, G. S. HAMILTON, D. A. SUTHERLAND, L. A. STEARNS, F. DAVIDSON, M. O. HAMMILL, G. B. STENSON, AND A. ROSING-ASVID, *Rapid circulation of warm subtropical waters in a major glacial fjord in East Greenland*, *Nature Geosci*, 3 (2010), pp. 182–186.

- [13] F. STRANEO AND P. HEIMBACH, *North Atlantic warming and the retreat of Greenland's outlet glaciers*, *Nature*, 504 (2013), pp. 36–43.
- [14] F. STRANEO, P. HEIMBACH, O. SERGIENKO, G. HAMILTON, G. CATANIA, S. GRIFFIES, R. HALLBERG, A. JENKINS, I. JOUGHIN, R. MOTYKA, W. T. PFEFFER, S. F. PRICE, E. RIGNOT, T. SCAMBOS, M. TRUFFER, AND A. VIELI, *Challenges to understanding the dynamic response of Greenland's marine terminating glaciers to oceanic and atmospheric forcing*, *Bulletin of the American Meteorological Society*, 94 (2013), pp. 1131–1144.
- [15] F. STRANEO, D. SUTHERLAND, D. HOLLAND, C. GLADISH, G. HAMILTON, H. JOHNSON, E. RIGNOT, Y. XU, AND M. KOPPES, *Characteristics of ocean waters reaching Greenland's glaciers*, *Annals of Glaciology*, 53 (2012), pp. 202–210.
- [16] D. A. SUTHERLAND, F. STRANEO, G. B. STENSON, F. J. DAVIDSON, M. O. HAMMILL, AND A. ROSING-ASVID, *Atlantic water variability on the SE Greenland continental shelf and its relationship to sst and bathymetry*, *Journal of Geophysical Research: Oceans*, 118 (2013), pp. 847–855.
- [17] N. WILSON, F. STRANEO, AND P. HEIMBACH, *Submarine melt rates and mass balance for Greenland's remaining ice tongues*, *The Cryosphere*, 2017 (in press, 2017), pp. 1–17.